NASA/TM—2000-209657 2000 022 240

IN-35

436791

pg 524

Rare Earth Optical Temperature Sensor

Donald L. Chubb and David S. Wolford
Glenn Research Center, Cleveland, Ohio

January 2000

The NASA STI Program Office . . . in Profile

Since its founding, NASA has been dedicated to the advancement of aeronautics and space science. The NASA Scientific and Technical Information (STI) Program Office plays a key part in helping NASA maintain this important role.

The NASA STI Program Office is operated by Langley Research Center, the Lead Center for NASA's scientific and technical information. The NASA STI Program Office provides access to the NASA STI Database, the largest collection of aeronautical and space science STI in the world. The Program Office is also NASA's institutional mechanism for disseminating the results of its research and development activities. These results are published by NASA in the NASA STI Report Series, which includes the following report types:

- TECHNICAL PUBLICATION. Reports of completed research or a major significant phase of research that present the results of NASA programs and include extensive data or theoretical analysis. Includes compilations of significant scientific and technical data and information deemed to be of continuing reference value. NASA's counterpart of peer-reviewed formal professional papers but has less stringent limitations on manuscript length and extent of graphic presentations.

- TECHNICAL MEMORANDUM. Scientific and technical findings that are preliminary or of specialized interest, e.g., quick release reports, working papers, and bibliographies that contain minimal annotation. Does not contain extensive analysis.

- CONTRACTOR REPORT. Scientific and technical findings by NASA-sponsored contractors and grantees.

- CONFERENCE PUBLICATION. Collected papers from scientific and technical conferences, symposia, seminars, or other meetings sponsored or cosponsored by NASA.

- SPECIAL PUBLICATION. Scientific, technical, or historical information from NASA programs, projects, and missions, often concerned with subjects having substantial public interest.

- TECHNICAL TRANSLATION. English-language translations of foreign scientific and technical material pertinent to NASA's mission.

Specialized services that complement the STI Program Office's diverse offerings include creating custom thesauri, building customized data bases, organizing and publishing research results . . . even providing videos.

For more information about the NASA STI Program Office, see the following:

- Access the NASA STI Program Home Page at ***http://www.sti.nasa.gov***

- E-mail your question via the Internet to help@sti.nasa.gov

- Fax your question to the NASA Access Help Desk at (301) 621-0134

- Telephone the NASA Access Help Desk at (301) 621-0390

- Write to:
  NASA Access Help Desk
  NASA Center for AeroSpace Information
  7121 Standard Drive
  Hanover, MD 21076

ERRATA

NASA/TM—2000-209657

Rare Earth Optical Temperature Sensor

Donald L. Chubb and David S. Wolford

January 2000

On the report documentation page (Standard Form 298), block 5 should read

WU–632–6A–1A–00

NASA/TM—2000-209657

Rare Earth Optical Temperature Sensor

Donald L. Chubb and David S. Wolford
Glenn Research Center, Cleveland, Ohio

National Aeronautics and
Space Administration

Glenn Research Center

January 2000

Available from

NASA Center for Aerospace Information
7121 Standard Drive
Hanover, MD 21076
Price Code: A03

National Technical Information Service
5285 Port Royal Road
Springfield, VA 22100
Price Code: A03

RARE EARTH OPTICAL TEMPERATURE SENSOR

Donald L. Chubb and David S. Wolford
National Aeronautics and Space Administration
Glenn Research Center
Cleveland, Ohio 44135

A new optical temperature sensor suitable for high temperatures (≥1700 K) and harsh environments is introduced. The key component of the sensor is the rare earth material contained at the end of a sensor that is in contact with the sample being measured. The measured narrow wavelength band emission from the rare earth is used to deduce the sample temperature. A simplified relation between the temperature and measured radiation was verified experimentally. The upper temperature limit of the sensor is determined by material limits to be approximately 2000 °C. The lower limit, determined by the minimum detectable radiation, is found to be approximately 700 K. At high temperatures 1 K resolution is predicted. Also, millisecond response times are calculated.

I. INTRODUCTION

There are a limited number of temperature sensors suitable for high temperatures (>1500 °C) and harsh environments. Platinum-rhodium type thermocouples,[1] which can operate in reactive environments, are suitable for temperatures up to 1700 °C. However, similar to all thermocouples, they are not suitable for electrically hostile-environments. For temperatures beyond 1700 °C radiation thermometers[1] are generally used. However, radiation thermometers require knowledge of the emissive properties of the sample being measured. For a sample with constant emittance (gray body) a radiation thermometer can be used without knowing the emittance.[1] However, for a sample with an emittance that depends on the wavelength, a radiation thermometer is not suitable.

In this paper we report on a new optical temperature sensor suitable for high temperatures and harsh environments. This sensor does not require knowledge of the emissive properties of the sample being measured. The key to the operation of this sensor is the narrow band emission exhibited by rare earth ions (Re) such as ytterbium (Yb) and erbium (Er), in various host materials. Depending on the host material this sensor will operate at temperatures greater than 1700 °C.

Most atoms and molecules at solid state densities emit radiation in a continuous spectrum much like a blackbody. However, the rare earths, even at solid state densities, emit radiation in narrow bands much like an isolated atom. The reason this occurs is the following. For doubly (Re^{++}) and triply charged (Re^{+++}) ions of these elements in crystals the orbits of the valence 4f electronics, which accounted for visible and near infrared emission and absorption, lie inside the 5s and 5p electron orbits. The 5s and 5p electrons "shield" the 4f valence electronics from the surrounding ions in the crystal. As a result, the rare earth ions in the solid state emit in narrow bands, much like the radiation from an isolated atom. The rare earths of most interest for the optical temperature sensor have emission bands in the near infrared ($800 \leq \lambda \leq 3000$ nm).

Development of the rare earth optical temperature sensor has resulted from research on rare earth containing selective emitters for thermophotovoltaic (TPV) energy conversion.[2] In that research we have found that rare earth doped yttrium aluminum garnet ($Re_xYt_{3-x}Al_5O_{12}$) where Re=Yb,Er,Tm or Ho is an excellent selective emitter. It is chemically stable at high temperatures (>1500 C) and produces emittances of $\varepsilon(\lambda) \approx 0.7$ in the emission bands.

In the following section the theory of the operation of the sensor is presented. Following that discussion, experimental results verifying the sensor operation will be presented. In the final section conclusions will be drawn.

II. THEORY OF OPERATION

Figure 1 is a schematic drawing for the rare earth optical temperature sensor. The sensor consists of 5 components; a rare earth containing end piece, an optical fiber, a narrow band optical filter, an optical detector, and electronics to convert the detector output to a temperature. The rare earth containing end piece, which is in contact with the sample to be measured, is attached to the optical fiber. Radiation from an emission band of the rare earth, which is proportional to the sample temperature, passes through the optical fiber to the bandpass filter. The narrow band filter transmits to the detector only wavelengths within the emission band of the rare earth. Output from the detector is then converted to a temperature by an analog electronics package.

The upper temperature limit for this sensor will be determined by the temperature limits of the materials. If ytterbia (Yb_2O_3), which has a melting point of 2227 °C is used for the emitting end of the optical fiber then temperatures ≈2000 °C should be possible if a yttria (Y_2O_3, melting point = 2410 °C) optical fiber is used. If a sapphire (Al_2O_3) optical fiber is used then the upper limit is reduced since the melting point of sapphire is 2072 °C. These materials are chemically stable in atmosphere at high temperature.

A. Relation Between Temperature and Detector Output

Assuming the rare earth containing end piece emits uniformly over the area of the fiber, A_ℓ, the radiation power, $q_s(\lambda,T_s)$ entering the optical fiber from the rare earth at wavelength, λ, is the following.

$$q_s(\lambda, T_s) = \varepsilon_b(\lambda) e_B(\lambda, T_s) A_\ell \quad \mathrm{W/nm} \tag{1}$$

Where $\varepsilon_b(\lambda)$ is the hemispherical spectral emittance into the optical fiber and $e_B(\lambda,T_s)$ is the blackbody emissive power[3] at the temperature, T_s, of the rare earth containing end piece.

$$e_B(\lambda, T_s) = \frac{2\pi c_1}{\lambda^5\left[\exp(c_2/\lambda T_s) - 1\right]} \quad \mathrm{W/nm \cdot cm^2} \tag{2}$$

$$c_1 = hc_o^2 = 5.9544 \times 10^{15} \quad \mathrm{W \cdot nm^4/cm^2} \tag{3a}$$

$$c_2 = hc_o/k = 14.388 \times 10^6 \quad \mathrm{nmK} \tag{3b}$$

Where c_o is the speed of light in vacuum, h is Plank's constant and k is Boltzmann's constant.

We assume that the emission band of the rare earth is wider than the bandwidth ($\lambda_u \le \lambda \le \lambda_\ell$) of the optical filter. In other words, $\varepsilon_b(\lambda) > 0$ for $\lambda_u \le \lambda \le \lambda_\ell$. Also, the transmittance of the optical filter, $\tau_f(\lambda) = 0$ for $\lambda_u > \lambda > \lambda_\ell$ Therefore, if the optical filter transmittance is $\tau_f(\lambda)$, then the power impinging on the detector, $q_d(\lambda,T_s)$, is the following.

$$q_d(\lambda, T_s) = \tau_f(\lambda)\tau_\ell(\lambda)\varepsilon_b(\lambda)e_B(\lambda, T_s)A_\ell F_{\ell d} \quad \lambda_u \le \lambda \le \lambda_\ell \tag{4a}$$

$$q_d(\lambda, T_s) = 0 \quad \lambda_u > \lambda > \lambda_\ell \tag{4b}$$

The term $F_{\ell d}$ is the fraction ($F_{\ell d} \le 1$) of the radiation that leaves the end of the optical fiber and reaches the detector. It is a geometrical factor that does not depend on λ or T_s and is called the view factor or configuration factor[3] for the fiber to the detector. Included in $\tau_\ell(\lambda)$ is the loss of radiation that escapes out the sides of the optical fiber, as well as, absorption losses.

In using equation (4) for the radiation power arriving at the detector the following approximations are being made.

(1) radiation leaving rare earth containing end piece is uniform across A_ℓ.
(2) The filter transmittance, τ_f, optical fiber transmittance, τ_ℓ, and the spectral emittance, ε_b, depend only on wavelength.
(3) Only radiation originating from the rare earth end piece reaches the detector.

If the rare earth containing end piece is of uniform thickness and at a uniform temperature in the direction parallel to the surface of the end piece then approximation 1 will be applicable. Since $q_s(\lambda,T_s)$ is small absorption in the optical filter and fiber will be small so that τ_f and τ_ℓ will be independent of $q_s(\lambda, T_s)$ and depend only on λ. However, if a significant temperature drop ($\Delta T/T_s > .05$) occurs across the rare earth containing end piece then ε_b will be a function of T_s, as well as, λ.[2] To minimize this effect the rare earth containing end piece must be thin (≤0.05 cm), but not too thin. The emittance, ε_b, depends on the film thickness.[2] If the film is too thin (<0.005 cm) the emittance will be reduced to a value such that q_s is too small to be detected. The indices of refraction of the optical fiber and rare earth containing end piece will change slightly with temperature. We neglect this effect on ε_b and τ_ℓ.

If the sample being measured has large emittance within the emittance band of the rare earth then this sample radiation will contribute to q_s. This background radiation can be eliminated by placing a low emittance material such as platinum (Pt) between the sample and the rare earth containing end piece. In the experiment to be discussed in the next section, Pt foil was placed between the sample and the rare earth containing end piece. Any radiation, that impinges on the sides of the optical fiber will not reach the detector. This radiation will merely pass through the fiber in wavelength regions where the fiber is transparent or be absorbed in wavelength regions of high absorption ($\lambda > 5000$ nm for sapphire). None of this radiation will be refracted such that it can reach the detector as long as the index of refraction of the fiber is greater than the index of refraction of the surroundings.

Now consider the relation between the detector output and the temperature, T_s. A photovoltaic (PV) detector, such as silicon, is used to convert the radiation input into a current output. A photoconductive detector could also be used as the optical detector. However, a silicon PV detector was chosen because of its superior detectivity, time constant and low cost.[4] The equivalent circuit[5] for a photovoltaic device is shown in figure 2. The current generated by the input radiation is i_{ph}, the current that flows if a potential V is applied when the device is in the dark is i_{dark} and the output current that flows through the load is i. The series resistance is R_s and the shunt resistance is R_{sh}. Applying Kirchhoff's Law to the circuit loop containing R_s and R_{sh} yields the following.

$$i = \frac{R_{sh}\left(i_{ph} - i_{dark}\right) - V_L}{R_{sh} + R_s} \tag{5}$$

The dark current is the following.[5]

$$i_{dark} = i_{sat}\left[\exp(aV/T_d) - 1\right] \qquad a = \frac{e}{k} = 8.62 \times 10^{-5}\,\frac{V}{K} \tag{6}$$

Where i_{sat} is the so-called saturation current, e is the electric charge and T_d is the temperature of the device. Since $V = V_L + iR_s$ equation (5) becomes the following.

$$i = \frac{1}{R_{sh} + R_s}\left\{R_{sh}\left[i_{ph} - i_{sat}\left(\exp(aV_L/T_d)\exp(ai\,R_s/T_d) - 1\right)\right] - V_L\right\} \tag{7}$$

Since this current output will be feed into an operational amplifier that acts like a short circuit ($V_L = 0$), the current is the following.

$$i_{sc} = \frac{R_{sh}}{R_{sh} + R_s}\left\{i_{ph} - i_{sat}\left[\exp(ai_{sc}R_s/T_d) - 1\right]\right\} \tag{8}$$

We now assume that the photovoltaic detector has very small series resistance ($R_s \to 0$). This is a good approximation for silicon detectors.[5] In that case the exponential term in equation (8) goes to one. Therefore, the short circuit output current equals the photon generated current.

The photon generated current is given by the following equation.[5]

$$i_{sc} = i_{ph} = \int_{\lambda_u}^{\lambda_\ell} Sr(\lambda) q_d(\lambda, T_s)\, d\lambda \tag{10}$$

Appearing in equation (10) is the spectral response of the PV detector, $Sr(\lambda)$, which gives the current generated per unit of radiation power incident on the PV detector. In using equation (10) we are assuming that the PV detector responds to all radiation within the limits ($\lambda_u \le \lambda \le \lambda_\ell$) of the optical filter. In other words, $Sr(\lambda) > 0$ for $\lambda_u \le \lambda \le \lambda_\ell$.

Substituting equation (4a) in equation (10) yields the following result for i_{sc}.

$$i_{sc}(T_s) = A_\ell F_{\ell d}\int_{\lambda_u}^{\lambda_\ell} \tau_f(\lambda)\tau_\ell(\lambda)\varepsilon_b(\lambda)Sr(\lambda)e_B(\lambda, T_s)d\lambda \tag{11}$$

To proceed further we must have information on the wavelength dependence of τ_f, τ_ℓ, ε_b and Sr. The most simplification occurs if the bandwidth of the optical filter is so small that τ_f, τ_ℓ, ε_b, Sr and e_B are constant for $\lambda_u \le \lambda \le \lambda_\ell$. In that case equation (11) becomes the following.

$$i_{sc}(T_s) = A_\ell F_{\ell d}\tau_f\tau_\ell\varepsilon_b Sr\left[\frac{2\pi c_1}{\exp(c_2/\lambda_f T_s)-1}\right]\left[\frac{\lambda_\ell - \lambda_u}{\lambda_f^5}\right] \tag{12}$$

Where $\lambda_f = (\lambda_u + \lambda_\ell)/2$ is the center wavelength of the optical filter. For most all applications $\lambda_f < 2000$ nm and $T_s < 2500$ K. Therefore, $c_2/\lambda_f T_s > 2.88$ and $\exp[c_2/\lambda_f T_s] >> 1$. Also, $A_d F_{d\ell} = A_\ell F_{\ell d}{}^3$, where A_d is the detector area and $F_{d\ell}$ is the detector to optical fiber view factor. In that case equation (12) becomes the following.

$$i_{sc}(T_s) = 2\pi c_1 A_d F_{d\ell}\tau_f\tau_\ell\varepsilon_b Sr\left[\frac{\lambda_\ell - \lambda_u}{\lambda_f^5}\right]\exp[-c_2/\lambda_f T_s] \tag{13}$$

Solving this equation for $1/T_s$ yields the following result.

$$\frac{1}{T_s} = \frac{\lambda_f}{c_2}[\ln C - \ln i_{sc}(T_s)] \tag{14}$$

Where,

$$C = 2\pi c_1 A_d F_{d\ell}\tau_f\tau_\ell\varepsilon_b Sr\left[\frac{\lambda_\ell - \lambda_u}{\lambda_f^5}\right] \tag{15}$$

The constant C, which is independent of T_s, can be determined by a calibration procedure. At some known calibration temperature, T_c, the short circuited current $i_{sc}(T_c)$ is measured. Therefore,

$$\ln C = \frac{c_2}{\lambda_f T_c} + \ln i_{sc}(T_c) \tag{16}$$

and

$$T_s = \left[\frac{1}{T_c} + \frac{\lambda_f}{c_2}\left\{\ln[i_{sc}(T_c)] - \ln[i_{sc}(T_s)]\right\}\right]^{-1} \tag{17}$$

Therefore, with the appropriate analog electronics the measured short circuit current, i_{sc}, of the PV detector can be converted to a temperature, T_s.

Remember that equation (17) was derived assuming that τ_f, τ_ℓ, ε_b and Sr are constants for $\lambda_u \le \lambda \le \lambda_\ell$. This is a good approximation for the optical fiber transmittance, τ_ℓ. The reason being that the most probable optical fibers for high temperature are sapphire or yttria (Yt_2O_3) which have nearly constant transmittance for wavelengths of interest ($800 \le \lambda \le 2000$ nm). It is not a good approximation to assume τ_f, ε_b and Sr are independent of λ. However, as shown in appendix A where wavelength dependence of τ_f, ε_b and Sr is included the short circuit current, i_{sc}, can be closely approximated by the following expression.

$$i_{sc} = C_o \exp[-c_2/\lambda_f T_s] \tag{18}$$

Where C_o is independent of T_s and depends on $\tau_f(\lambda)$, $\varepsilon_b(\lambda)$ and $Sr(\lambda)$, where λ_f is the center wavelength of the optical filter. As a result, equation (17) applies even when wavelength dependence of τ_f, ε_b and Sr are included. If the bandwidth, $\Delta\lambda_f$, of the optical filter is too large ($\Delta\lambda_f > 25$ nm) then C_o will depend on T_s. Therefore, making $\Delta\lambda_f$ small results in C_o being nearly independent of T_s. For a hypothetical sensor that uses a ytterbium containing emitter, which has an emission band centered at $\lambda_E = 955$ nm, and an optical filter with $\lambda_f = 950$ nm and $\Delta\lambda_f = 10$ nm the parameter C_o varies less than 0.65 percent for $620 \leq T_s \leq 2500$ K. If the filter bandwidth $\Delta\lambda_f = 25$ nm then C_o varies less than 3.0 percent for the same temperature range. As the results in Appendix A show the variation in C_o for high temperatures ($1220 \leq T_s \leq 2500$ K) is much less. For the $\Delta\lambda_f = 10$ nm filter the variation is less than 0.1 percent and for the $\Delta\lambda_f = 25$ nm filter the variation is less than 0.5 percent.

B. Temperature Error

Consider the temperature error that results from using equation (18) for the short circuit current. Let $i_{sct}(T_{st})$ be the short circuit current corresponding to the true temperature, T_{st}. Let $i_{sce}(T_{se})$ be the short circuit current that has a corresponding temperature, T_{se}, and is in error from the true short circuit current, i_{sct}, by the factor, p. As a result the following expression applies.

$$i_{sce}(T_{se}) = p\, i_{sct}(T_{st}) \tag{19}$$

Using equation (19) and equation (17) the following result is obtained for the error in temperature, $(T_{st} - T_{se})/T_{st}$.

$$\frac{T_{st} - T_{se}}{T_{st}} = \frac{\frac{\lambda_f}{c_2} T_{st} \ln p}{\frac{\lambda_f}{c_2} T_{st} \ln p - 1}$$

And since $\lambda_f/c_2\, T_{st} \ln p << 1$,

$$\frac{T_{st} - T_{se}}{T_{st}} \approx -\frac{\lambda_f}{c_2} T_{st} \ln p \tag{20}$$

In the case of the $\Delta\lambda_f = 25$ nm and $\lambda_f = 950$ nm optical filter just discussed, the maximum error in i_{sc} that results from using equation (18) is less than 3 percent for $620 \leq T_s \leq 2500$ K. Therefore, p = 0.97 and

$$\frac{T_{st} - T_{se}}{T_{st}} < 2.0 \times 10^{-6} T_{st} \qquad \begin{array}{c} 620 \leq T_s \leq 2500 \text{ K} \\ \lambda_f = 950 \text{ nm}, \Delta\lambda_f = 25 \text{ nm} \end{array} \tag{21}$$

Therefore, if $T_{st} = 2500$ K then $T_{st} - T_{se} < 12.6$ K is the maximum possible error in T_s for $\Delta\lambda_f = 25$ nm optical filter for $620 \leq T_s \leq 2500$ K. For the $\Delta\lambda_f = 10$ nm and $\lambda_f = 950$ nm optical filter the maximum error in i_{sc} is less than 0.65 percent for $620 \leq T_s \leq 2500$ K. Therefore, p = 0.9935 and

$$\frac{T_{st} - T_{se}}{T_{st}} < 4.3 \times 10^{-7} T_{st} \qquad \begin{array}{c} 620 \leq T_s \leq 2500 \text{ K} \\ \lambda_f = 950 \text{ nm}, \Delta\lambda_f = 10 \text{ nm} \end{array} \tag{22}$$

For $T_{st} = 2500$ K the maximum possible error in T_s is $T_s - T_{se} < 2.7$ K. If we restrict the temperature range to $1220 \leq T_s \leq 2500$ K then p = 0.995 for the $\Delta\lambda_f = 25$ nm filter and p = 0.999 for the $\Delta\lambda_f = 10$ nm filter. As a result the following results are obtained.

$$T_{st} - T_{se} < 2.1\text{K} \qquad \begin{matrix} \lambda_f = 950\text{ nm}, \Delta\lambda_f = 25\text{ nm} \\ T_{st} = 2500\text{K} \end{matrix} \tag{23a}$$

$$T_{st} - T_{se} < 0.4\text{K} \qquad \begin{matrix} \lambda_f = 950\text{ nm}, \Delta\lambda_f = 10\text{ nm} \\ T_{st} = 2500\text{K} \end{matrix} \tag{23b}$$

From these results we conclude that temperature errors resulting from the use of equation (18) for i_{sc} will be less than 1K for a temperature sensor that uses the λ_f = 950 nm, $\Delta\lambda_f$ = 10 nm filter over most of the useful temperature range.

C. Temperature Limits

What is the useful temperature range of the sensor? The upper temperature limit is set by the durability of the material and has already been discussed. However, the lower temperature limit is set by the minimum short circuit current, i_{sc}, that can be measured. To estimate this lower temperature limit we make use of the results of appendix A. Assume that the optical filter and Yb containing emitter have the following characteristics, λ_f = 950 nm, $\Delta\lambda_f$ = 10 nm, τ_{fMAX} = 0.35, λ_E = 955 nm, ε_{MAX} = 0.8, ε' = 0.01. Also assume a silicon detector of 1 mm in diameter (r_d = 0.05 cm) and maximum spectral response $Sr(\lambda_g)$ = 0.5 A/W, where λ_g = 1100 nm is the wavelength that corresponds to the silicon bandgap energy, E_g = 1.1eV. In addition, assume the optical fiber transmittance is τ_ℓ = 0.2 and the optical fiber diameter is approximately the same as the detector diameter and is as close as possible to the detector so that the detector to optical fiber view factor is $F_{d\ell} \approx 0.5$. In that case the results from appendix A yield C_o = 5.8 A. The minimum value i_{sc} that can be detected will be determined by the electronics package and the electronic noise in the system. Using operational amplifiers[6] in the electronics package should allow minimum short circuit currents of $i_{sc} = 10^{-8}$ A to be easily detected. In that case with C_o = 5.8 A and λ_f = 950 nm equation (18) yields T_s = 750 K. Obviously, at a given temperature a larger value of $\Delta\lambda_f$ will result in larger C_o and therefore larger i_{sc}. Thus, for $\Delta\lambda_f$ = 25 nm with all other conditions the same yields C_o = 13.8 A and a temperature limit of T_s = 720 K. However, it must be remembered that $\Delta\lambda_f$ = 25 nm results in a larger error in T_s than the $\Delta\lambda_f$ = 10 nm case.

Based on the results just discussed, a lower temperature limit of the order of 700 K should be possible with a silicon detector and optical fiber of 1 mm diameter. Using a larger diameter optical fiber and detector will result in a lower temperature limit. However, the larger optical fiber will also result in a larger temperature error since thermal conduction away from the sample will be larger.

D. Response Time

The time behavior of the output of the rare earth containing end piece of the sensor, q_s, depends on how fast the end piece reaches a steady state temperature after a change in the sample temperature, $T_s(t)$. This response time, τ, will be much larger than the transmission time of q_s through the optical fiber and filter since they occur at the speed of light. The response time of the detector and electronics should also be much smaller than τ. Therefore, the response time of the end piece, τ, will determine the response time of the sensor.

Assume the end piece behaves in a one-dimensional manner so that its temperature is governed by the one-dimensional heat conduction equation.

$$k_{th}\frac{\partial^2 T}{\partial x^2} + \rho c_p \frac{\partial T}{\partial t} = 0 \tag{24}$$

Where t is time, x is the coordinate perpendicular to cross sectional area, A_ℓ, of the end piece, k_{th} is the thermal conductivity, ρ is the density and c_p is the specific heat. If equation (24) is written in dimensionless form using dimensionless length $\bar{x} = x/d$, where d = thickness of the end piece then we find that the appropriate dimensionless time is $\bar{t} = t/\tau_0$ where,

$$\tau_o = \frac{\rho c_p d^2}{k_{th}} \tag{25}$$

In reference 7 solutions to equation (24) are presented for various boundary conditions and initial conditions. In all cases the time dependence is the following, where α is a constant.

$$T \sim e^{-\alpha t/\tau_o} \tag{26}$$

This same result can be obtained by using the method of separation of variables on equation (24). The constant α depends on the boundary conditions and is the order of 1. Therefore, equation (25) can be used to estimate the response time, τ, of the sensor.

As equation (25) indicates the response time is a quadratic function of d so that by making the end piece thin the response time will be small. Assume that the end piece is a rare earth oxide such as ytterbia (Yb_2O_3) or erbia (Er_2O_3). Then $\rho < 10$ gm/cm^3 and $c_p < 1$ J/gmK.[8] There is no data available on the thermal conductivity, k_{th}, or the rare earth oxides at high temperature. However, we expect they will have low thermal conductivity at high temperature similar to other ceramic materials such as alumina where $k_{th} \approx 0.1$ W/cmK. Therefore, assume $k_{th} \geq 0.05$ W/cmK so that equation (25) yields the following for the response time, τ.

$$\tau < 200 \ d^2 \text{ sec} \qquad d \text{ in cm} \tag{27}$$

Thus, if the minimum thickness end piece is d = 0.005 cm then the response time is $\tau < 5$ msec. As discussed earlier, the response time of the sensor should be determined by the end piece response time, τ.

III. EXPERIMENTAL VERIFICATION OF SENSOR OPERATION

To verify that equation (17) applies for determining the temperature, T_s, the experiment shown in figure 3 was used. The sensor consists of a 0.055 cm diameter sapphire fiber with an erbium aluminum garnet ($Er_3Al_5O_2$) emitter of thickness, d = 0.03 cm attached with platinum (Pt) foil. Erbium has an emission band at $\lambda \approx 1000$ nm. The Pt foil serves two purposes. First of all it holds the emitter to the end of the fiber and secondly it blocks all radiation from the sample being measured. The thin ($\approx$0.005 cm) Pt foil will produce negligible temperature change between the sample and the emitter. In this case the sample being measured is Pt foil with a type R platinum versus platinum (13 percent) rhodium thermocouple attached behind the Pt foil. The Pt sample is held with an alumina holder, which is located in the center of a high temperature atmospheric furnace. At the other end of the sapphire fiber is a chopper and monochromator, which serves as the optical filter with a bandwidth of $\Delta\lambda_f \approx 2$ nm. A silicon detector converts the radiation leaving the monochromator to a short circuit current, i_{sc}, which is measured with a lock-in amplifier.

The experimental procedure to verify equation (17) was as follows. First i_{sc} (T_c) was determined by measuring i_{sc} when the thermocouple was at temperature T_c. Knowing $i_{sc}(T_c)$, T_c and $\lambda_f = 1012$ nm, equation (17) was then used to calculate T_s for a series of different thermocouple temperatures, T_{TC}. If equation (17) is valid then $T_s = T_{TC}$. In figure 4 the sample temperature, T_s, calculated from equation (17) is plotted as a function of the thermocouple temperature, T_{TC}, for two different ranges. In figure 4(a) the range is $863 \leq T_{TC} \leq 1430$ K and in figure 4(b) the range is $1334 \leq T_{TC} \leq 1879$ K.

As figure 4 shows the agreement between T_s and T_{TC} is excellent. The largest error, $err = |T_{TC} - T_s|/T_{TC}$, occurs at the lowest temperatures. For figure 4(a), $err_{MAX} = 0.03$ and for figure 4(b), $err_{MAX} = 0.008$. As a result of this close agreement between T_s and T_{TC} we conclude that equation (17) is valid for determining the sample temperature, T_s, from the measured short circuit current, i_{sc}.

Figure 5 shows the lock-in amplifier output, which is directly proportional to the short circuit current, i_{sc}, as a function of T_s for the same conditions as figure 4(b). Two things should be noted. First of all, because of the exponential dependence of i_{sc} on T_s (eq. (18)) the sensor sensitivity increases with temperature. As figure 5 shows for high temperatures (>1100K) a small change in T_s results in a several millivolt change in amplifier output. Thus, we expect 1K temperature resolution at high temperature. The second thing to note is even though the monochromator bandwidth is small ($\approx$2 nm), the amplifier output is many millivolts. Therefore, the electronic circuit that converts i_{sc} to T_s (eq. (17)) will operate with a large input signal, which should eliminate electronic noise problems.

IV. CONCLUSION

The operation of the rare earth optical temperature sensor has been experimentally verified. For the temperature range $863 \leq T \leq 1430$K the maximum temperature deviation of the sensor temperature from a measured thermocouple temperature was 3 percent. For the temperature range $1334 \leq T \leq 1879$K this error was reduced to 0.8 percent. Calculations show that a simple relation (eq. (18)) between temperature and detector output can be used to determine the temperature. The error resulting from using this relation will be less than 1K.

Material durability limits the upper temperature of the sensor. Using a yttria optical fiber and rare earth oxide emitters the upper temperature limit should be approximately 2000 °C. The lower temperature limit is determined by the minimum signal that can be detected. This limit is calculated to be approximately 700 K if a silicon detector is used.

Response time of the detector will be determined by how fast the emitter responds to a temperature change. This response time was estimated using the equation for thermal conduction. Results indicate that response times the order of msec are possible. Because of the exponential dependence of sensor output on the temperature we expect temperature resolution of 1 K to be possible.

The electronics package to convert the sensor output to a temperature is under development. This electronics package can be designed using commercially available parts. Thus the most expensive component of the sensor is expected to be the optical fiber.

APPENDIX A. RELATION BETWEEN TEMPERATURE AND DETECTOR SHORT CIRCUIT CURRENT

The complete relationship between the sample temperature, T_s, and the PV detector short circuit current is given by equation (11).

$$i_{sc}(T_s) = 2\pi c_1 A_\ell F_{\ell d} \int_{\lambda_u}^{\lambda_\ell} \tau_f(\lambda)\tau_\ell(\lambda)\varepsilon_b(\lambda)Sr(\lambda)\frac{d\lambda}{\lambda^5\left[\exp(c_2/\lambda T_s)-1\right]} \tag{11}$$

As stated in the discussion about equation (17), it is a good approximation to assume the optical fiber transmittance, $\tau_\ell(\lambda)$, is constant for $\lambda_u \le \lambda \le \lambda_\ell$. The spectral response of a PV detector can be approximated as a linear function of wavelength.[9]

$$Sr(\lambda) = \frac{\lambda}{\lambda_g} Sr_g \quad \frac{A}{W} \qquad 0 \le \lambda \le \lambda_g$$

$$Sr(\lambda) = 0 \qquad \lambda_g < \lambda$$

Where Sr_g is the spectral response at $\lambda = \lambda_g = hc_o/E_g$ and E_g is the bandgap energy of the PV detector. A linear approximation can also be used for the spectral emittance, $\varepsilon_b(\lambda)$, of the rare earth selective emitter[2] for a narrow wavelength region around an emission band centered at $\lambda = \lambda_E$ that is located within the transmission band $\lambda_u \le \lambda \le \lambda_\ell$ of the optical filter.

$$\varepsilon_b(\lambda) = \varepsilon_{MAX} - \varepsilon'(\lambda_E - \lambda) \qquad \lambda_u \le \lambda \le \lambda_E$$

$$\varepsilon_b(\lambda) = \varepsilon_{MAX} - \varepsilon'(\lambda - \lambda_E) \qquad \lambda_E \le \lambda \le \lambda_\ell$$

Where $\varepsilon_{MAX} = \varepsilon(\lambda_E)$ is the maximum emittance and ε' is the slope of the linear $\varepsilon_b(\lambda)$ versus λ approximation. For a narrow bandwidth interference filter the transmittance, $\tau_f(\lambda)$, can be closely approximated by a Gaussian function.

$$\tau_f(\lambda) = \tau_{fMAX} \exp\left\{-\ln 2\left[\frac{2(\lambda-\lambda_f)}{\Delta\lambda_f}\right]^2\right\} \tag{A3}$$

Where λ_f is the center wavelength of the transmission band, $\tau_{fMAX} = \tau_f(\lambda_f)$, and $\Delta\lambda_f$ is the bandwidth defined by the wavelengths $\lambda_{fu} = \lambda_f - \Delta\lambda_f/2$ and $\lambda_{f\ell} = \lambda_f + \Delta\lambda_f/2$ where $\tau_f(\lambda_f \pm \Delta\lambda_f/2) = \tau_{f\,MAX}/2$. Figure A1 compares the experimental transmittance of an interference filter with $\lambda_f = 949$ nm and $\Delta\lambda_f = 14$ nm with equation (A3). As can be seen the agreement is quite good.

Figure A2 shows the approximations for $Sr(\lambda)/Sr_g$, $\varepsilon_b(\lambda)/\varepsilon_{MAX}$, and $\tau_f(\lambda)/\tau_{fMAX}$ given by equations (A1), (A2) and (A3) for the case where $\lambda_f = 950$ nm, $\Delta\lambda_f = 10$ nm, $\lambda_E = 955$ nm, $\varepsilon_{MAX} = 0.8$, $\varepsilon_\lambda' = 0.01\ nm^{-1}$ (ytterbium) and $\lambda_g = 1100$ nm (silicon). These approximations were used in equation (11) and i_{sc} was calculated by numerical integration. The integration limits were $\lambda_u = \lambda_f - 4\Delta\lambda_f$ and $\lambda_\ell = \lambda_f + 4\Delta\lambda_f$, which insures that at these limits the integrand in equation (11) vanishes. To determined if equation (18) is a valid approximation for i_{sc} we calculated C_o in equation (18).

$$C_o = i_{sc} \exp\left[c_2/\lambda_f T_s\right] \tag{A4}$$

Where i_{sc} in equation (A4) is obtained by numerical integration of equation (11).

Figure A3(a) shows C_o as a function of T_s for the $\Delta\lambda_f = 10$ nm filter ($\lambda_f = 950$ nm, $\tau_{fMAX} = 0.35$), fiber transmittance, $\tau_\ell = 0.2$ and the ytterbium emitter ($\lambda_E = 955$ nm, $\varepsilon_{MAX} = 0.8$, $\varepsilon_\lambda' = 0.01\ nm^{-1}$) and silicon detector

($\lambda_g = 1100$ nm, $Sr_g = 0.5$ A/W). As can be seen, C_o changes only by a small amount for $620 \leq T_s \leq 2500$ K. Thus, C_o is nearly independent of T_s and equation (18) is a valid approximation for i_{sc}. Figure A3(b) shows C_o for the case where $\Delta\lambda_f = 25$ nm with all other conditions being the same as in figure A3(a). In this case C_o changes more than the $\Delta\lambda_f = 10$ nm case, but equation (18) should still be a good approximation for i_{sc}. If the optical filter and emission band are matched ($\lambda_f = \lambda_E$) then C_o varies even less over the temperature range ($620 \leq T_s \leq 2500$ K). For the $\Delta\lambda_f = 10$ nm filter the maximum variation in C_o is less than 0.65 percent if $\lambda_E = 955$ nm and $\lambda_f = 950$ nm but is only 0.33 percent if $\lambda_f = \lambda_E = 955$ nm.

REFERENCES

1. Schooley, J.F., "Thermometry," CRC Press, Boca Raton, Florida, 1986, Ch. 6.
2. Chubb, D.L., Pal, A.T., Patton, M.O., and Jenkins, P.P., J. European Ceramic Soc., 19, 2551, (1999), also NASA TM–1999-208491.
3. Siegel, R. and Howell, J.R., "Thermal Radiation heat Transfer," 2nd edition, Washington, DC, Hemisphere, 1981, Ch. 2, 3 and 7.
4. Moore, J.H., Davis, C.C., and Coplan, M.A., "Building Scientific Apparatus, A Practical Guide to Design and Construction," Addison-Wesley, Reading, MA, 1983, Ch. 4.8.
5. Sze, S.M., "Physics of Semiconductor Devices," Wiley-Interscience, New York, 1969, Ch. 12.
6. Horowitz, P. and Hill, W., "The Art of Electronics," 2nd ed., New York, Cambridge University Press, 1989, Ch. 4.
7. Carslaw, H.S. and Jaeger, J.C., "Conduction of Heat in Solids," 2nd ed., Oxford University Press, 1959, Ch. 3.
8. Lide, D.R. (Ed.), CRC Handbook of Chemistry and Physics," 71st ed., CRC Press, 1990.
9. Green, M.A., "Solar Cells, Operating Principles Technology and System Applications," Prentice-Hall Series in Solid State Physical Electronics, 1982, Ch. 8.

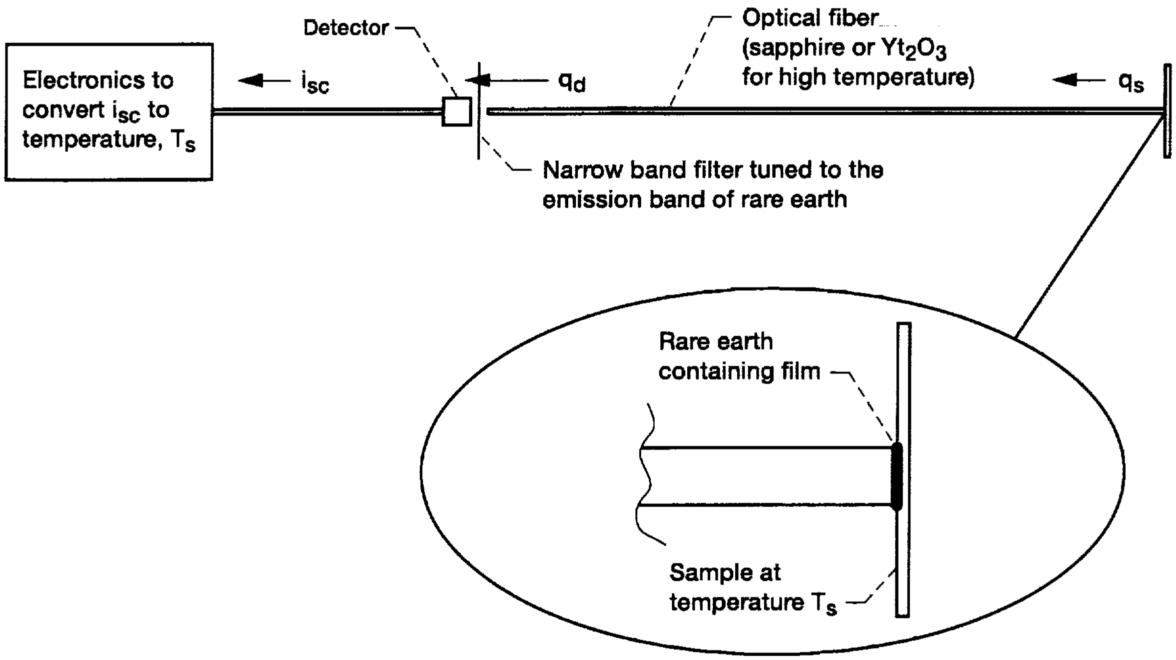

Figure 1.—Schematic of rare earth optical temperature sensor.

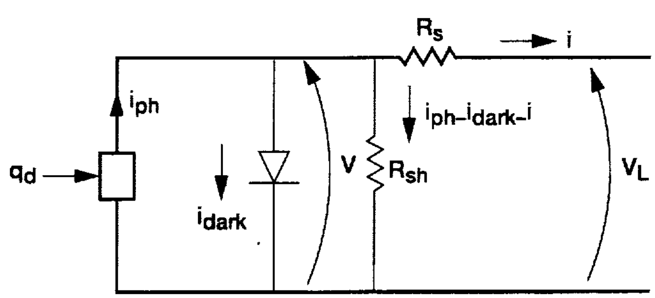

Figure 2.—Equivalent circuit for photovoltaic device.

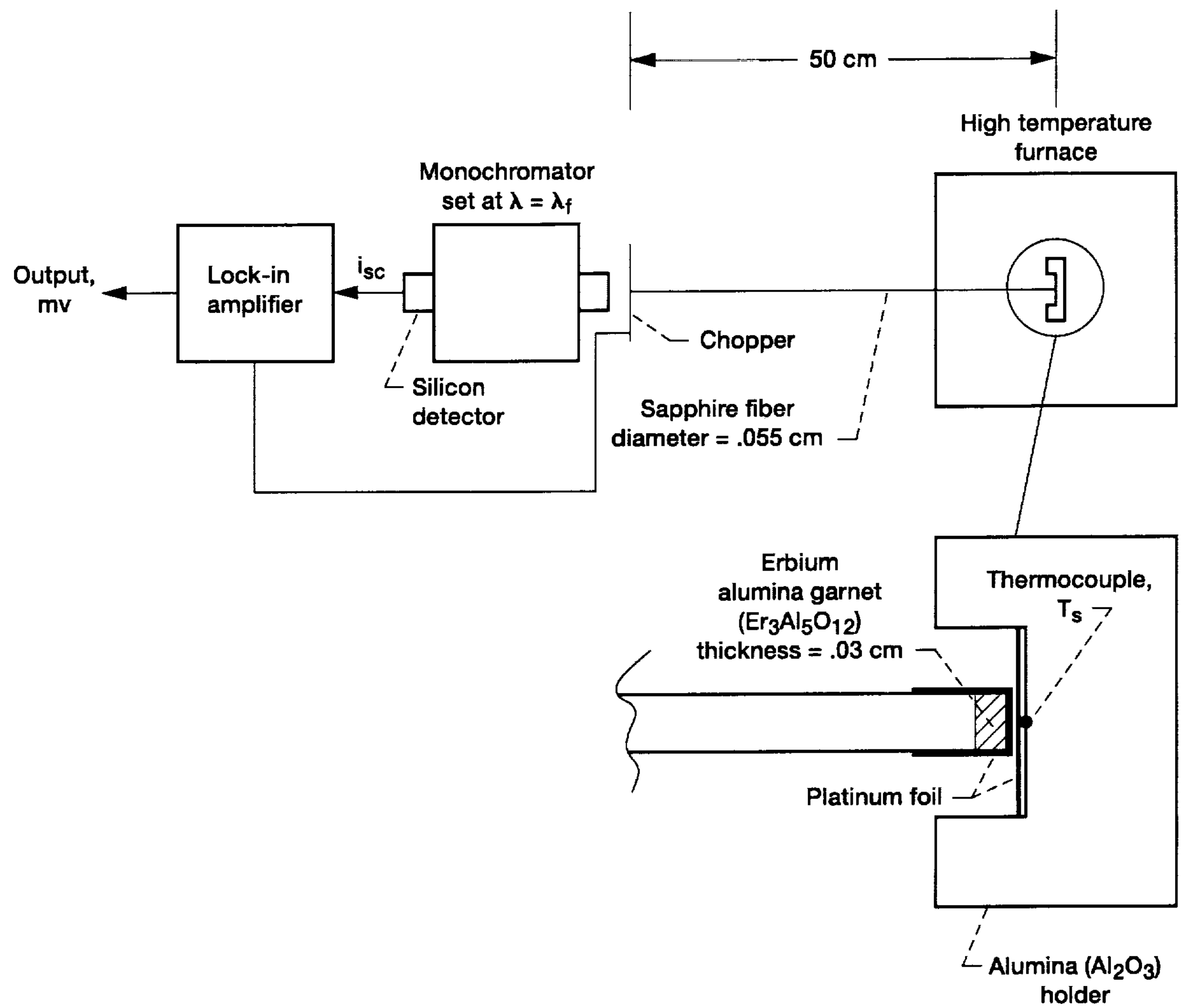

Figure 3.—Experiment to verify rare earth optical temperature sensor operation.

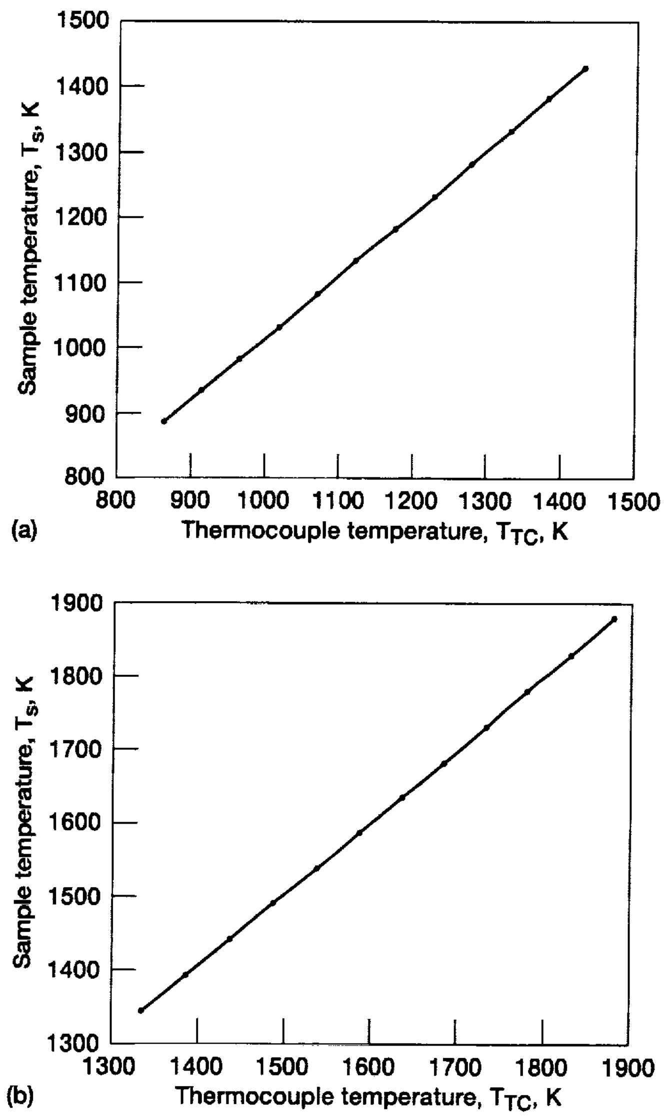

Figure 4.—Comparison of sample temperature, T_s, determined using equation (17) for erbium aluminum garnet emitter, and sample temperature measured by type R thermocouple, T_{TC}. Center wavelength, $\lambda_f = 1012$ nm. (a) $863 \leq T_{TC} \leq 1430$ K, $T_C = 1430$ K. (b) $1334 \leq T_{TC} \leq 1879$ K, $T_C = 1879$ K.

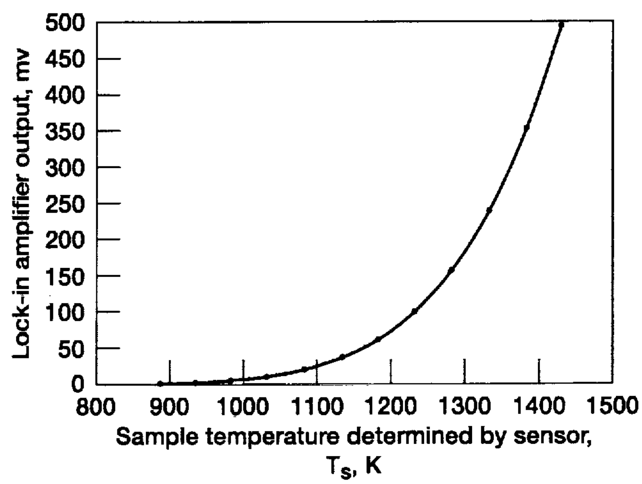

Figure 5.—Lock-in amplifier output, which is directly proportional to short circuit current, i_{SC}, of silicon detector, as a function of the measured sample temperature, T_S, for same conditions as figure 4(a).

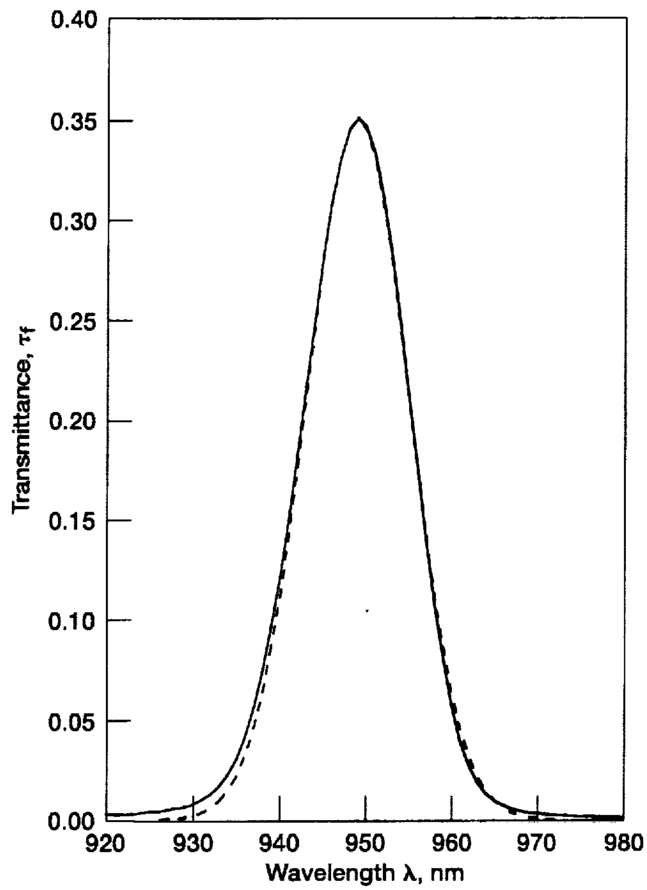

Figure A1.—Comparison of actual transmittance, τ_f, with Gaussian approximation of τ_f for narrow bandwidth interference filter with center wavelength, $\lambda_f = 949$ nm and bandwidth, $\Delta\lambda_f = 14$ nm. Actual τ_f is solid line and Gaussian approximation is dashed line.

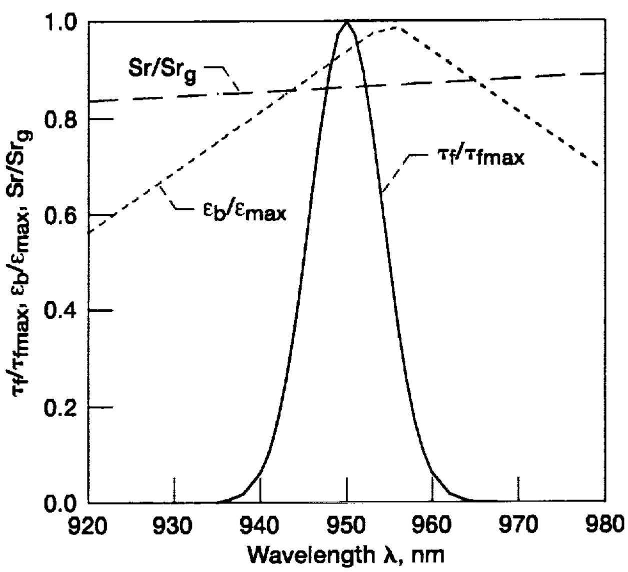

Figure A2.— Optical filter transmittance, τ_f/τ_{fmax}, Yb emitter emittance, $\varepsilon_b/\varepsilon_{max}$, and silicon detector spectral response, Sr/Sr_g used to calculate the parameter C_o in eq. (18).

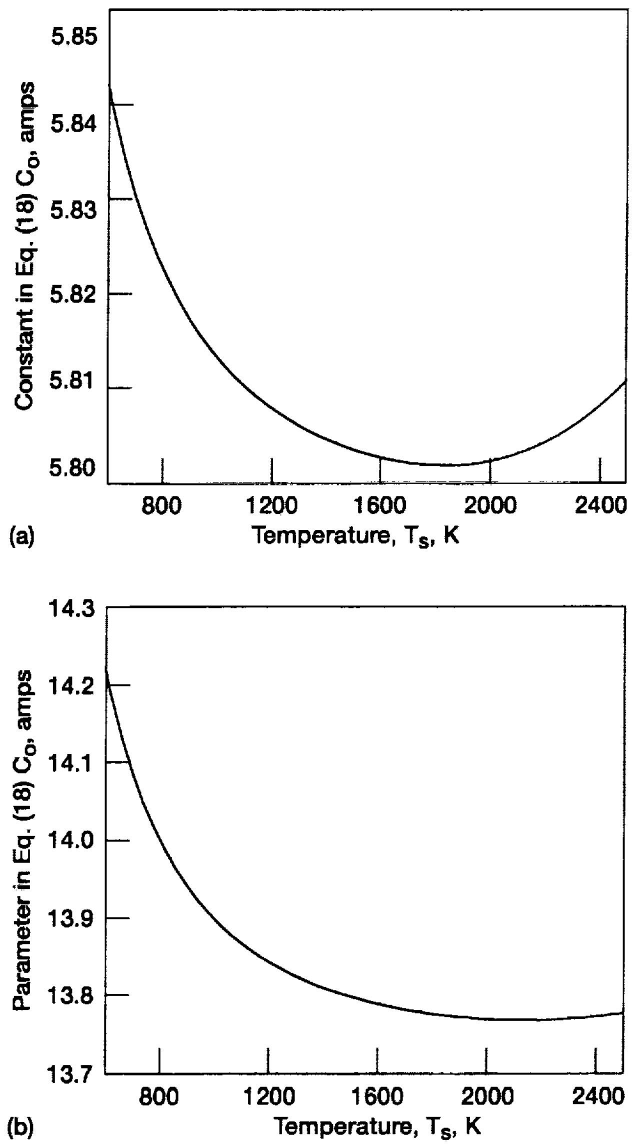

Figure A3.— Parameter in Eq. (18) as a function of temperature for the following conditions, r_d = .05 cm, F_{dl} = .5, τ_l = .2, τ_{fmax} = .35, ε_{max} = .8, ε' = .01 nm^{-1}, λ_g = 1100 nm, Sr_g = .5 A/W. (a) Filter center wavelength, λ_f = 950 nm, bandwith, $\Delta\lambda_f$ = 10 nm. (b) Filter center wavelength, λ_f = 950 nm, bandwith, $\Delta\lambda_f$ = 25 nm.

REPORT DOCUMENTATION PAGE

Form Approved
OMB No. 0704-0188

1. AGENCY USE ONLY (*Leave blank*)	2. REPORT DATE	3. REPORT TYPE AND DATES COVERED
	January 2000	Technical Memorandum

4. TITLE AND SUBTITLE

Rare Earth Optical Temperature Sensor

5. FUNDING NUMBERS

WU–632–1A–1A–00

6. AUTHOR(S)

Donald L. Chubb and David S. Wolford

7. PERFORMING ORGANIZATION NAME(S) AND ADDRESS(ES)

National Aeronautics and Space Administration
John H. Glenn Research Center at Lewis Field
Cleveland, Ohio 44135–3191

8. PERFORMING ORGANIZATION REPORT NUMBER

E–11970

9. SPONSORING/MONITORING AGENCY NAME(S) AND ADDRESS(ES)

National Aeronautics and Space Administration
Washington, DC 20546–0001

10. SPONSORING/MONITORING AGENCY REPORT NUMBER

NASA TM—2000-209657

11. SUPPLEMENTARY NOTES

Responsible person, Donald L. Chubb, organization code 5410, (216) 433–2242.

12a. DISTRIBUTION/AVAILABILITY STATEMENT

Unclassified - Unlimited
Subject Categories: 35 and 74 Distribution: Nonstandard

This publication is available from the NASA Center for AeroSpace Information, (301) 621–0390.

12b. DISTRIBUTION CODE

13. ABSTRACT ***(Maximum 200 words)***

A new optical temperature sensor suitable for high temperatures (≥1700 K) and harsh environments is introduced. The key component of the sensor is the rare earth material contained at the end of a sensor that is in contact with the sample being measured. The measured narrow wavelength band emission from the rare earth is used to deduce the sample temperature. A simplified relation between the temperature and measured radiation was verified experimentally. The upper temperature limit of the sensor is determined by material limits to be approximately 2000 °C. The lower limit, determined by the minimum detectable radiation, is found to be approximately 700 K. At high temperatures 1 K resolution is predicted. Also, millisecond response times are calculated.

14. SUBJECT TERMS

Temperature sensor, Selective emitter, Rare earth, Optical fiber

15. NUMBER OF PAGES

24

16. PRICE CODE

A03

17. SECURITY CLASSIFICATION OF REPORT	18. SECURITY CLASSIFICATION OF THIS PAGE	19. SECURITY CLASSIFICATION OF ABSTRACT	20. LIMITATION OF ABSTRACT
Unclassified	Unclassified	Unclassified	

NSN 7540-01-280-5500

Standard Form 298 (Rev. 2-89)
Prescribed by ANSI Std. Z39-18
298-102